Ion-dependent Inactivation of Barium Current through L-type Calcium Channels

Gonzalo Ferreira, Jianxun Yi, Eduardo Ríos, and Roman Shirokov

From the Department of Molecular Biophysics and Physiology, Rush University, Chicago, Illinois 60612

ABSTRACT It is widely believed that Ba^{2+} currents carried through L-type Ca^{2+} channels inactivate by a voltage-dependent mechanism similar to that described for other voltage-dependent channels. Studying ionic and gating currents of rabbit cardiac Ca^{2+} channels expressed in different subunit combinations in tsA201 cells, we found a phase of Ba^{2+} current decay with characteristics of ion-dependent inactivation. Upon a long duration (20 s) depolarizing pulse, I_{Ba} decayed as the sum of two exponentials. The slow phase ($\tau \approx 6$ s, 21°C) was parallel to a reduction of gating charge mobile at positive voltages, which was determined in the same cells. The fast phase of current decay ($\tau \approx 600$ ms), involving about 50% of total decay, was not accompanied by decrease of gating currents. Its amplitude depended on voltage with a characteristic U-shape, reflecting reduction of inactivation at positive voltages. When Na^+ was used as the charge carrier, decay of ionic current followed a single exponential, of rate similar to that of the slow decay of Ba^{2+} current. The reduction of Ba^{2+} current during a depolarizing pulse was not due to changes in the concentration gradients driving ion movement, because Ba^{2+} entry during the pulse did not change the reversal potential for Ba^{2+}. A simple model of Ca^{2+}-dependent inactivation (Shirokov, R., R. Levis, N. Shirokova, and E. Ríos. 1993. *J. Gen. Physiol.* 102:1005–1030) robustly accounts for fast Ba^{2+} current decay assuming the affinity of the inactivation site on the α_1 subunit to be 100 times lower for Ba^{2+} than Ca^{2+}.

KEY WORDS: gating current • signal transduction • cardiac muscle • heterologous expression

INTRODUCTION

Brief openings of L-type Ca^{2+} channels cause the increases in intracellular Ca^{2+} concentration required to effect rapid metabolic switching in a variety of cellular processes (Tsien and Tsien, 1990). The Ca^{2+} signalling process is controlled and limited by multi-layered inactivation mechanisms, that affect the plasmalemmal as well as the intracellular release Ca^{2+} channels. Channel inactivation sharpens the kinetics and temporal precision of the signals, and prevents longer term increases in $[Ca^{2+}]_i$, which, among other problems, lead to stimulation of intracellular proteolysis (Turner et al., 1988).

In L-type and other Ca^{2+} channels (Tareilus et al., 1994; Cox and Dunlap, 1994), inactivation is produced by two mechanisms. One is mediated by the calcium ions that carry the current (Brehm and Eckert, 1978; Eckert and Chad, 1984), and it appears to involve binding to a site highly specific for Ca^{2+}. In L-type channels the site is located near the channel mouth (Imredy and Yue, 1992, 1994; Shirokov et al., 1993), on the main (α_1) channel protein (Neely et al., 1994), and has been equated with an EF hand-like portion of the cytoplasmic COOH terminus (De León et al., 1995).

The other mechanism of inactivation does not require the passage of current (Fox, 1981). It is linked to the change in transmembrane potential, and is accompanied by changes in gating currents, which are broadly termed inactivation of charge (Shirokov et al., 1992). The two mechanisms function independently, as demonstrated by the fact that changes in $[Ca^{2+}]_i$ (Hadley and Lederer, 1991) and Ca^{2+} current through the channels (Shirokov et al., 1993) do not affect gating currents.

Parallel recording of gating currents and ion currents helped elucidate voltage-dependent aspects of Ca^{2+} channel gating (Field et al., 1988; Bean and Ríos, 1989; Hadley and Lederer, 1989) but is complicated in native cells by the presence of substantial Na^+ channel gating current. The present work overcomes this problem using tsA201 cells, an expression system virtually free of endogenous channels. With Ba^{2+} as the permeant ion, we compared inactivation of gating charge with decay of ion currents, under the prevailing hypothesis that inactivation of L-type channel current is exclusively voltage-dependent in the absence of Ca^{2+} (e.g., Kass and Sanguinetti, 1984). The results disproved this hypothesis, favoring instead a dual mechanism of inactivation.

Dr. Ferreira's permanent address is Dept. Biofisica, Facultad de Medicina, Montevideo, Uruguay. Dr. Shirokov's permanent address is A.A. Bogomoletz Institute of Physiology, Kiev, Ukraine.

Address correspondence to Roman Shirokov, Department of Molecular Biophysics and Physiology, Rush University School of Medicine, 1750 W. Harrison St., Suite 1279JS, Chicago, IL 60612. Fax: 312-942-8711; E-mail: rshiroko@rush.edu

METHODS

Preparation of Transfected and Native Cells

Experiments were performed in the large T antigen–transformed human embryonic kidney cells (tsA201 line) grown in DME medium (Sigma Chemical Co., St. Louis, MO) supplemented with 10% FBS (BioWhittaker, Walkersville, MD) and 1% penicillin/streptomycin (Sigma) in 5% CO_2. Cardiac rabbit α_{1C}, rat brain β_{2a}, and rabbit skeletal muscle $\alpha_2\delta$ cDNAs were cloned in pCR3, pCMV, and pMT2 plasmid vectors respectively. High purity ($A_{260}/A_{280} \geq 1.95$) large-scale plasmid preparations were obtained using standard protocols (Qiagen Inc., Chadworth, CA). Transfections were done with 30 μg of each expression plasmid in different combinations (α_{1C}, $\alpha_{1C} + \beta_{2a}$, and $\alpha_{1C} + \beta_{2a} + \alpha_2\delta$) using a modified calcium phosphate precipitation method (Chien et al., 1995) in 100-mm tissue culture dishes. Cells were incubated with DNA for 6–8 h and then were shocked with 10% DMSO for 8 min. After the shock, cells were transferred onto glass coverslips, fed with fresh media and incubated until further evaluation. Electrophysiological recordings were made within 24–48 h post-transfection on round nonclustered cells. No sizable ionic or gating currents were observed in tsA201 cells in the absence of transfection. After transfection, the fraction of cells selected and patched that had Ca^{2+} currents was 60–80%. Recording of native Ca^{2+} currents was carried out in single rabbit cardiac ventricular myocytes, which were obtained by an enzymatic dissociation method (modified from Mitra and Morad, 1985) from young (1,500 g) male mutt rabbits.

Electrophysiological Recording

Cells were placed in small chambers (<200 μl) and perfused by continuous flow of external solutions. Records were obtained by a standard whole-cell patch clamp procedure using an Axopatch 200A amplifier and a 16-bit A/D-D/A converter card (HSDAS 16; Analogic Corp., Peabody, MA) under a 486 PC computer. Patch electrodes had resistances of 1.5–4 MΩ. Whole-cell capacitance, calculated as the area under a linear capacitive transient elicited by a −10 mV pulse, was 6–40 pF. Capacitance and resistance compensations were routinely done, and the charging time constant was typically 100 μs. Ionic currents were sampled at 0.15–1 kHz and gating currents at 10–40 kHz, depending on pulse duration.

All the currents represented are asymmetric, obtained after subtraction of scaled control currents, and not corrected for baselines. The control currents were elicited by pulses from −90 to −110 mV before each depolarization and after holding the cell at −90 mV for 30 s. All experiments were carried out at room temperature (~20°C).

Exponential Fitting and Statistics

Data are presented as averages ± SEM. Signficance of differences between mean values was evaluated by Student's *t* test. Time course of current decay was fitted (using a nonlinear least-squares routine) by the function $Y_1 = b + a \exp(-t/\tau)$ or the function $Y_2 = b + a_{slow} \exp(-t/\tau_{slow}) + a_{fast} \exp(-t/\tau_{fast})$. A_{fast}, A_{slow}, and B are the best fit amplitude parameters, a_{fast}, a_{slow}, and b, normalized to their sum. A and B symbolize the normalized amplitudes in the single exponential fit. In all cases in which both fits converged, the statistical significance of the fit improvement provided by the two- exponential function Y_2 was evaluated. The test was based on the likelihood ratio statistic, $LRS = (ssr_1 - ssr_2)/\sigma^2$ (Hoel, 1971; Hui and Chandler, 1990), in which ssr_1 and ssr_2 are the sums of squares of the residuals for the two fits and σ^2 is the variance of the record. LRS has a χ^2 distribution with 2 degrees of freedom (the difference between the number of free parameters of Y_2 and Y_1). If the statistic exceeds 6.0, the improvement in fit provided by the two-exponential function is significant to better than 5%. σ^2 was estimated by $ssr_2/(N-5)$, which, being probably in excess, gave an underestimate of LRS.

Solutions

The internal solution contained (in mM): 150 CsOH (or NMG), 110 glutamate, 20 HCl, 10 HEPES, 5 MgATP, and 10 EGTA (pH adjusted to 7.6 by addition of CsOH). Osmolality of the internal solution was routinely measured and adjusted to 300–320 mosmole/kg.

External recording solutions contained (in mM): 160 TEA-Cl, 10 Tris, and either 10 $CaCl_2$ or 10 $BaCl_2$. Sodium external solution contained (in mM): 150 NaCl, 10 HEPES. In some experiments about 0.5 μM $CaCl_2$ was added to this solution to stabilize the patch seal. In gating current experiments, 10–20 μM $GdCl_3$ was added to the external solution with 10 mM Ca^{2+}. All external solutions were adjusted to pH 7.2 and 300–320 mosmole/kg.

RESULTS

Inactivation of Ba^{2+} Currents Had Two Distinct Kinetic Phases

The lack of substantial endogenous voltage-dependent ion currents in tsA201 cells allowed us to study the time course of decay of Ba^{2+} currents (I_{Ba}) during very long pulses (up to 40 s). Ca^{2+} and Ba^{2+} currents in a cell transfected with α_{1C} and β_{2a} cDNAs are illustrated in Fig. 1, *A* and *B*. As shown in panel *B*, and as described often for I_{Ca}, the time course of I_{Ba} decay was well fitted by a sum of two exponentials plus a constant (Y_2 in METHODS). The record and the best fit line are shown to overlap in the inset, where they are plotted semilogarithmically. The single exponential fit (*dashed line*) was poor.

Families of records from 33 cells were fitted with one and two-exponential functions. At voltages positive to +20 mV, 12 cells were discarded because they had a small outward steady current. Two other cells, which had unusually slow activation kinetics, were discarded because the two-exponential fit was not significantly better than the single exponential fit, as judged by the LRS. The averages of parameters obtained from the remaining 19 cells are in Fig. 1 *C*. On average, the time constant of the fast component of I_{Ba} decay (τ_{fast}) was minimal at +20 to +40 mV and increased (at a $P < 0.08$) at +60 mV. The amplitudes of the two exponentials (A_{slow} and A_{fast}) were comparable. A_{fast} went through a maximum at +20 mV, decaying at higher voltages. The slow component became faster and its amplitude greater at increasing depolarization. B decreased from 0.3 at −20 mV to 0.05 at +20 mV and increased to 0.15 at higher voltages. Because in the selected cells there was little if any outward current, even after 40 s pulses to +40 mV, and because neither current rundown nor substitution of NMG^+ for intracellular Cs^+ affected the decay parameters, these appear to

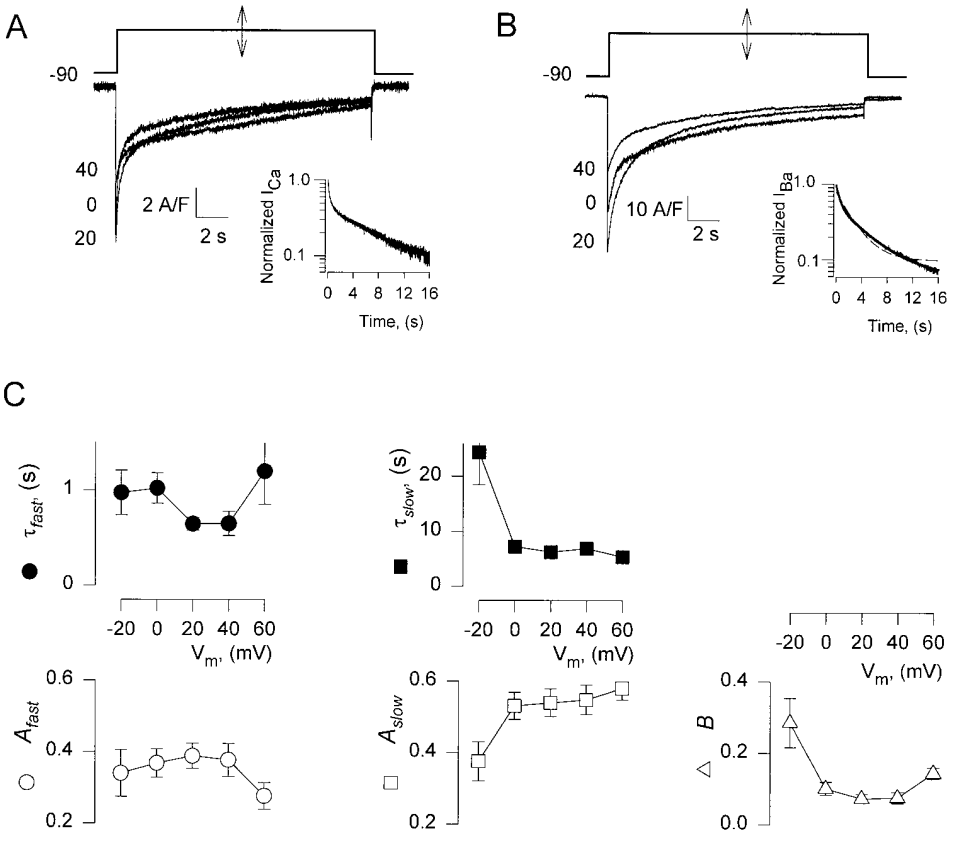

FIGURE 1. Kinetics of Ca^{2+} and Ba^{2+} currents. (*A*) Ca^{2+} currents elicited by depolarizing pulses of 16.5-s duration, from a holding potential of −90 mV to voltages indicated near the traces in mV. (*inset*) The current at +20 mV, normalized to peak value and plotted in semilog scale. (*B*) Ba^{2+} currents elicited by 16.5-s pulses. At membrane voltages from −20 to +60 mV I_{Ba} had a bi-exponential time course of decay. (*inset*) Semilog plot of I_{Ba} at +20 mV, normalized to its peak value. A sum of two exponentials fitted to $I_{Ba}(t)$ is represented by a continuous line superimposed to the data. The dashed line represents the best fit single exponential. The LRS (defined in METHODS) was 354.3, indicating significant improvement by the two-exponential fit. (*C*) Parameters, defined in METHODS, of the two-exponential fit to $I_{Ba}(t)$, ($n = 19$).

represent kinetics of the expressed channels. The crisp separation of the two decay phases and the observed differences in the dependencies of their parameters on voltage suggest the presence of two independent mechanisms of inactivation.

Only the Slow Phase of I_{Ba} Decay Was Accompanied by Reduction of Gating Charge

Using ionic current-blocking solutions we studied the effects of prolonged depolarization on the availability of gating currents associated with channel opening. The asymmetric (ON) charge transferred after the depolarizing transition of a 0.1 s pulse was equal to the (OFF) charge transferred upon repolarization. As expected from studies in native cells, prolonged depolarization reduced gating currents. This was demonstrated with one- and two-pulse protocols, to rule out errors due to ionic currents or fast recovery from inactivation of gating charge. Fig. 2 *A* shows the OFF transients obtained upon repolarization from +20 mV, after periods of depolarization indicated near the traces. The larger transient in each pair is the reference OFF after a 45-ms pulse (in every case preceding the prolonged depolarization). Surprisingly, reduction of charge transfer took much more time than decay of I_{Ba}. Fig. 2 *B* plots reduction of the OFF charge vs. pulse duration, averaged in nine cells. The curve is a single exponential fit ($\tau \approx 8$ s).

The reduction of the available charge after depolarization was also monitored by a double pulse protocol illustrated at top of Fig. 2 *C*. The membrane was conditioned at +20 mV, then it was repolarized to −60 mV for 7 ms and a test pulse to +50 mV was applied to move the charge available at voltages of channel opening. During conditioning depolarization currents were recorded at a low acquisition rate, which was increased at the repolarization swing. As in Fig. 2 *A*, the larger transient in each pair is the reference obtained before the corresponding conditioning pulse. The reduction in available charge is plotted vs. conditioning duration in 2 *D*. The reduction of gating charge at positive voltages had the same time course as the reduction of the OFF charge in the single pulse experiment.

Fig. 3 compares the time course of I_{Ba} decay and that of gating charge reduction. In the figure we superimposed data and fit of charge availability (from Fig. 2 *B*) on a record of I_{Ba} elicited by a 16.5 s depolarization. The exponential decay of charge availability (*solid curve*) has a time constant similar to that of the slow decay of I_{Ba}, suggesting that these are due to a slow inactivation mechanism, distinct and voltage-dependent. On the other hand, the figure clearly shows that about half of

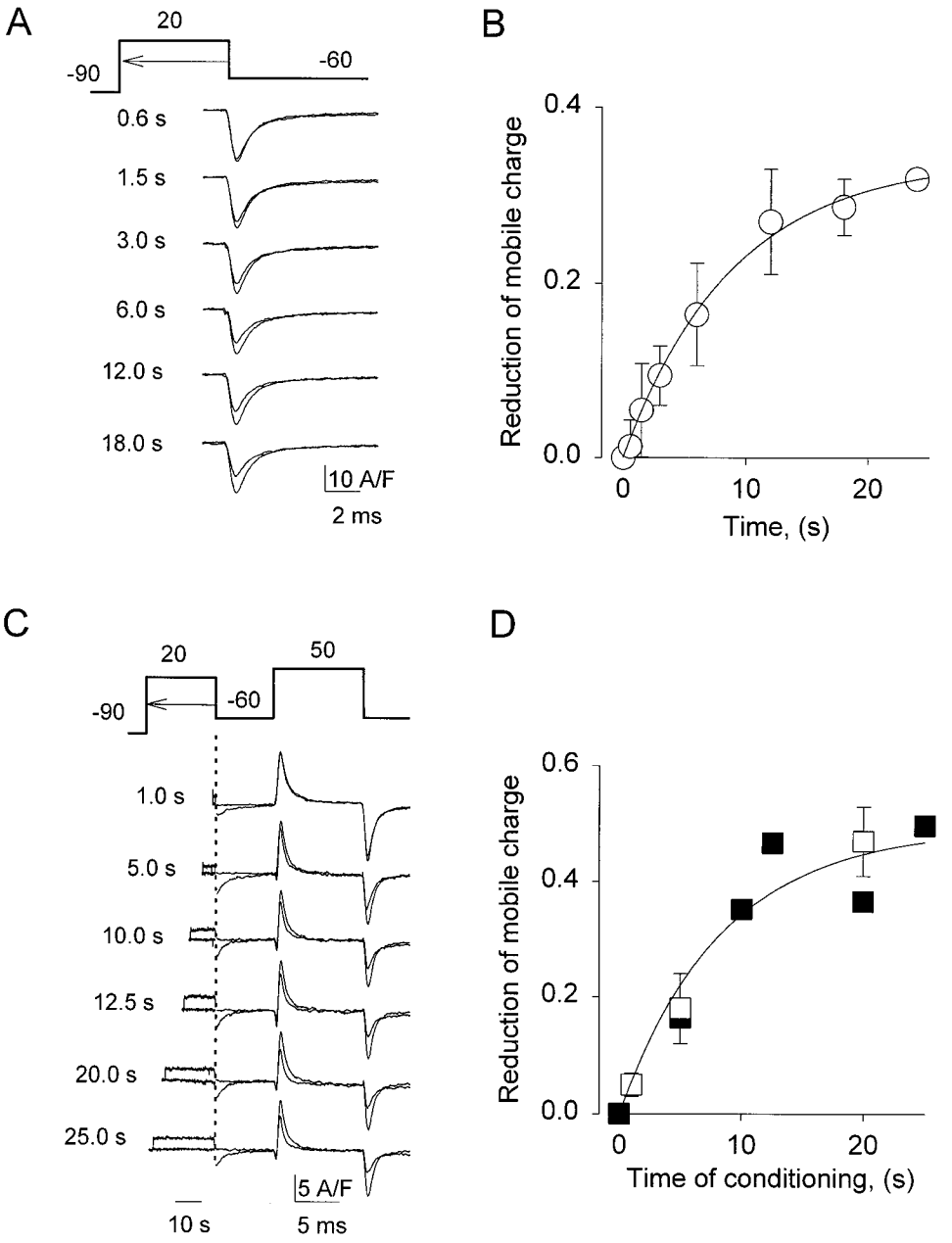

FIGURE 2. Reduction of mobile charge takes seconds. (*A*) OFF gating current transients after increasing times at +20 mV. The records are asymmetric currents obtained as described in METHODS. Durations of the test depolarizations that preceded the transients are listed near each plot. Test OFF transients are shown superimposed with larger reference transients, obtained at the trailing edge of 0.045-s pulses applied before each test depolarization. (*B*) Difference between reference and test OFF charge transfer, normalized to reference, vs. duration of depolarization at +20 mV (n = 9). The continuous line represents $\Delta Q_{max}(1 - \exp(-t/\tau))$, with ΔQ_{max} = 0.34 and τ = 8.7 s. (*C*) Gating currents elicited by a fixed test pulse after conditioning depolarizations of different durations (listed near each record). At left in the panel are the asymmetric currents during the conditioning depolarization, recorded at a slower sampling rate (up to the time indicated by the dotted line). Records obtained with and without conditioning pulse are shown superimposed. (*D*) Difference in ON charge transfer, reference minus conditioned, normalized to reference, vs. duration of the conditioning depolarization (*open symbols*, averages; n = 4; *filled symbols*, data from records in *C*). Continuous line generated as in *B*, with ΔQ_{max} = 0.49 and τ = 8.5 s.

the decay of I_{Ba} occurred much more rapidly than the process causing charge reduction. Indeed, as shown in Fig. 2 *A*, ON and OFF charges remained equal in single pulses of up to 1 s, a time at which ionic current had inactivated by ~40%.

Fast Decay of I_{Ba} Is a Current-dependent Process

Fast inactivation of I_{Ba} was studied with brief (0.3 s) test pulses to +20 mV, following a 2 s conditioning pulse to different voltages (which should cause fast inactivation almost exclusively) and a 1 s interpulse to −60 mV (to ensure the return of all intramembrane charge). Each pair of pulses was preceded by a single test pulse for reference, and the sets were applied at 1-min intervals. Reference and conditioned currents are shown in pairs in Fig. 4 *A*, normalized to correct for rundown. A conditioning pulse to 0 mV (eliciting substantial I_{Ba}) reduced the magnitude and the rate of decay of the following test current. Conditioning at +80 mV evoked no inward current and had less effect on the test current. Averages in seven cells are plotted vs. conditioning voltage in Fig. 4 *B*. Circles represent peak conditioning current relative to the maximal value at +10 mV and squares represent peak test current (measuring channel availability after conditioning). I_{Ba} appeared at −30 mV,

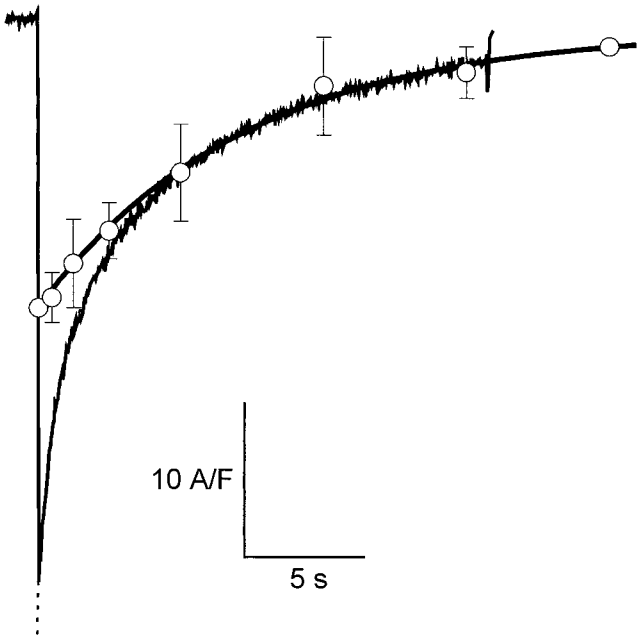

FIGURE 3. Slow inactivation of I_{Ba} and reduction of mobile charge had the same kinetics. Ba^{2+} current evoked by a 16.5-s pulse to +20 mV from a holding potential of −90 mV. Shown superimposed are the average values and fit (*thick line*) of charge reduction at +20 mV (same as in Fig. 2 *B*). Parameters of the two-exponential fit to the Ba^{2+} current (*dotted line*): $A_{fast} = 0.38$, $\tau_{fast} = 0.75$ s, $A_{slow} = 0.57$, $\tau_{slow} = 6.68$ s, $B = 0.05$.

peaked at +10 mV, and decayed at higher voltages. The availability had a U-shaped voltage dependence that mimicked the voltage dependence of the conditioning current, as befits a current- (rather than voltage-) dependent inactivation process (Tillotson, 1979). This inactivation was not due to Ca^{2+} contamination, as $[Ca^{2+}]$ was measured in the external solutions with a Ca^{2+} electrode and found to be negligible (<5 μM).

A U-shaped voltage dependence of the current availability could also be a manifestation of potentiation of channel activity by large positive pulses, as shown in snail neurons (Heyer and Lux, 1976), chromaffin cells (Hoshi et al., 1984), skeletal muscle (Sculptoreanu et al., 1993) and cardiac cells (Lee, 1987). However, the extent of current decay during the test pulses (*triangles* in Fig. 4 *B*) was minimal after conditioning at +10 mV and increased at more positive conditioning voltages. This implies that conditioning to a high voltage had a modest accelerating effect on the decay kinetics, which is against a major role of voltage-dependent potentiation, because in native cardiomyocytes potentiated currents had a much slower rate of decay (Lee, 1987). Also against voltage-dependent potentiation is the observation that the conditioned Ba^{2+} currents were never greater than reference currents, even after conditioning to +100 mV.

Fast Current Decay Was Absent when Na^+ Was the Permeant Ion

Fig. 5 shows representative records of Na^+ current (I_{Na}) through the α_{1C}/β_{2a} channels at submicromolar concentrations of extracellular divalent cations. The voltage dependence of I_{Na} (*diamonds* in Fig. 5 *B*) and its sensitivity to Ca^{2+} channel blockers were as described in native channels (Kostyuk et al., 1983; Hess et al., 1986), which proves that I_{Na} passed through the expressed L-type channels. In agreement with previous reports in isolated cardiac myocytes (Imoto et al., 1985; Hadley and Hume, 1987), I_{Na} activated at potentials about 30 mV more negative than I_{Ba} (*circles*). At all voltages I_{Na} decayed much more slowly than I_{Ba}. A scaled I_{Ba} trace plotted together with I_{Na} (Fig. 5 *C*) illustrates that the fast decay was absent when Ba^{2+} was removed. In fact, a fast component of decay was not resolvable even at very high densities of Na^+ current (up to 54 A/F). Including Ca^{2+} in the external solution at a concentration of 20 μM led to the appearance of a phase of I_{Na} decay with kinetics similar to those of the fast inactivation of I_{Ba} (Fig. 5 *C*).

Absence of Bulk Accumulation Effects

It is believed that the level of Ca^{2+} accumulation produced by typical membrane Ca^{2+} currents cannot significantly change the driving force that determines Ca^{2+} flux in a cell buffered with several mM of EGTA (Neher, 1986). The buffering capacity of such intracellular solutions will be lower for Ba^{2+} (because the affinity of EGTA for Ba^{2+} is about 100 times less than for Ca^{2+}; Harafuji and Ogawa, 1980). It is therefore conceivable that the current dependent reduction of I_{Ba} is due to a reduction of driving force on the ion upon accumulation of Ba^{2+} inside the cell. A simple single pool model of accumulation of Ba^{2+} in the volume of the cell, in which unidirectional Ba^{2+} fluxes are assumed to be independent, predicts first order decay of current, with rate constant proportional to initial current amplitude and to the reciprocal of cell volume. The volume of round cells (a good approximation for transfected tsA201 cells) is proportional to $C_m^{3/2}$, where C_m is membrane capacitance. Fig. 6 *A* plots τ_{fast}^{-1} vs. (peak $I_{Ba}/C_m^{3/2}$) at +20 mV for 21 cells, demonstrating no correlation between these variables.

The above test does not rule out depletion of Ba^{2+} ions outside the cell, or their accumulation in restricted spaces close to the conduction pathway. To test these possibilities we sought to demonstrate changes in the driving force for I_{Ba}, in experiments similar to those described in a study of Na^+ accumulation (Hadley and Hume, 1987) and illustrated in Fig. 6 *B*. I_{Ba} was elicited with a double pulse protocol similar to that in Fig. 4. The test pulse took the membrane to the reversal poten-

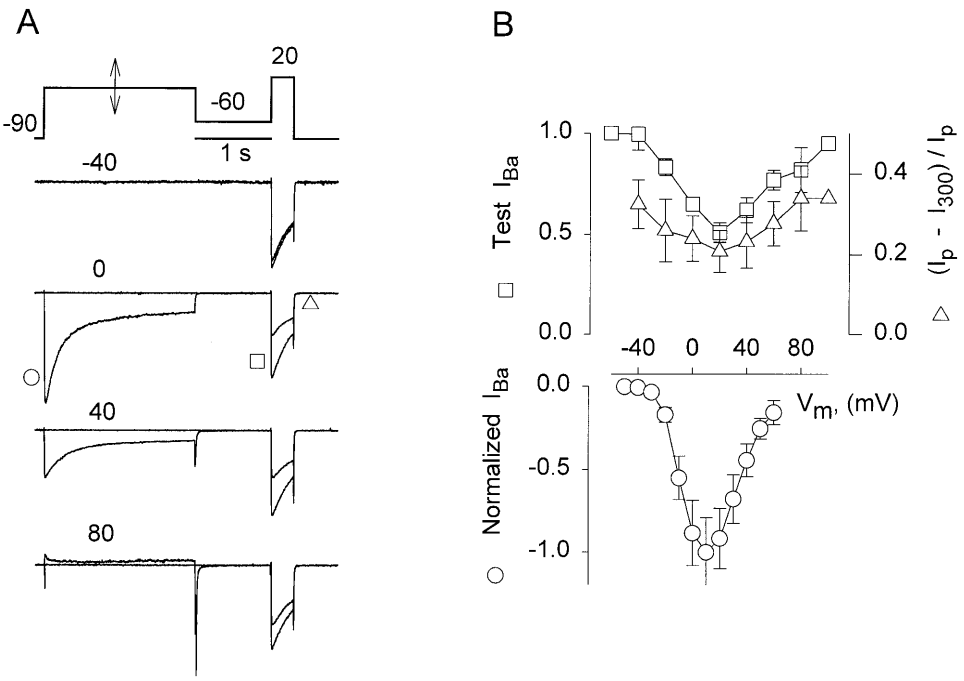

FIGURE 4. Availability of Ba^{2+} current after a brief conditioning pulse. (*A*) I_{Ba} elicited by a fixed test pulse after 2-s long conditioning pulses to different voltages (indicated in mV). Conditioned and reference current traces are shown superimposed. Within each pair, the currents are scaled to the peak of the reference current. Note symbols indicating measurements plotted in *B*. (*B*) *Squares*: peak of test I_{Ba} vs. conditioning voltage, (n = 7). *Triangles*: extent of inactivation of I_{Ba} during the test pulse, measured as $(I_{peak} - I\ (300\ ms))/I_{peak}$, ($n$ = 7). *Circles*: peak Ba^{2+} current during a pulse to the voltage in the abscissa, normalized in each cell to the maximum current (n = 19).

tial and elicited no net ionic current. If a large current preceding the test determined substantial accumulation and a change in driving force for Ba^{2+}, the conditioned pulse should elicit an outward current. Conditioning at 0 mV elicited near maximal I_{Ba} but did not result in the appearance of outward current during the test pulse. The decay in current can therefore be safely attributed to channel gating (inactivation) rather than a change in driving force.

Fast Decay Was Not due to Acidification

Ca^{2+} channel activity decreases at low intracellular pH (Kaibara and Kameyama, 1988) and EGTA is deproto-

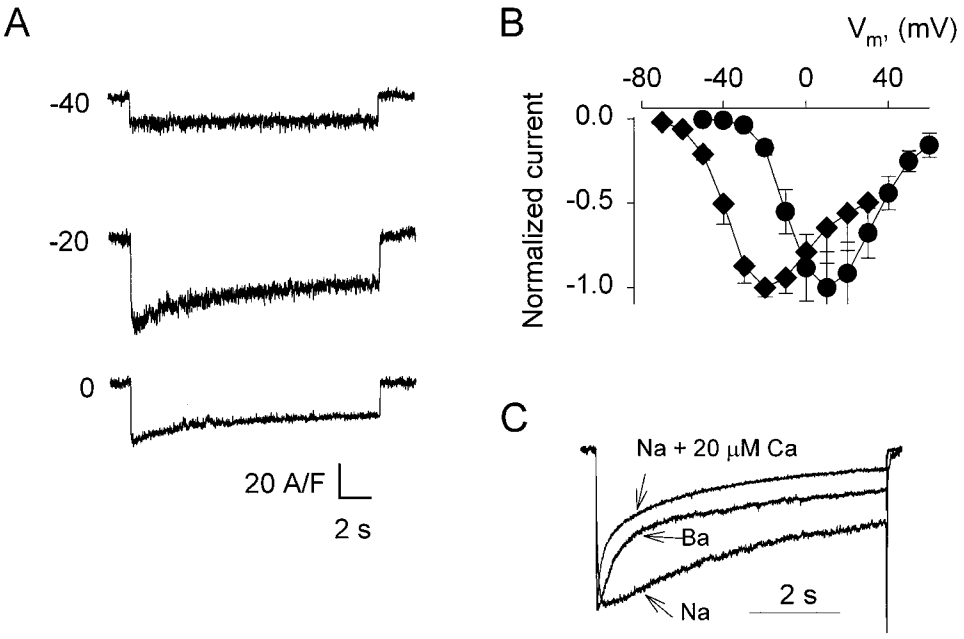

FIGURE 5. The fast component of inactivation was absent when Na^+ was the charge carrier. (*A*) Currents elicited in a Ca^{2+}-free, 150 mM Na^+ external solution by 16.5-s pulses to the voltages indicated in mV. (*B*) *Diamonds*: peak Na^+ current, normalized to its maximum in each cell, vs. pulse voltage (n = 5). *Circles*: peak current in 10 mM Ba^{2+} (n = 19). Peak I_{Na} was 25.6 ± 4.3 A/F, whereas peak I_{Ba} was 36 ± 3.5 A/F. (*C*) Currents obtained in different cells, in either 150 mM Na^+, 10 mM Ba^{2+}, or 150 mM Na^+ plus 20 μM Ca^{2+}, at the voltages of maximal currents. Records were scaled to the same amplitude. Parameters of a single exponential fit to the Na^+ current shown: A = 0.62, τ = 8.72 s, B = 0.38; two-exponential fits to Na^+ + 20 μM Ca^{2+}: A_{fast} = 0.43; τ_{fast} = 0.35 s, A_{slow} = 0.47, τ_{slow} = 5.84 s, B = 0.10; to Ba^{2+} current: A_{fast} = 0.46; τ_{fast} = 0.93 s, A_{slow} = 0.42, τ_{slow} = 12.63 s, B = 0.12. Note that the parameter values of the Na^+ + 20 μM Ca^{2+} fit are not significantly different from the average values for I_{Ba} in α_1/β cells (Table I).

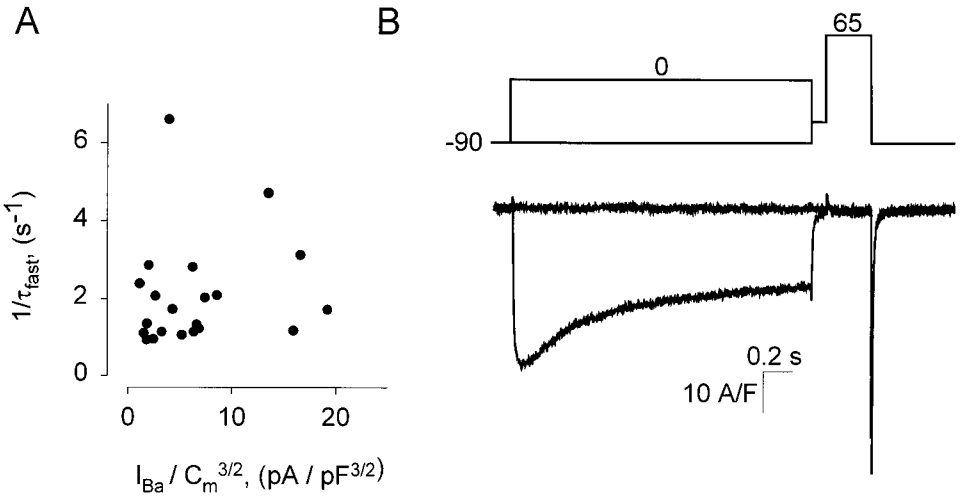

FIGURE 6. Two tests of Ba^{2+} accumulation. (*A*) Rate constant of fast decay of Ba^{2+} currents elicited at different voltages in different cells vs. the ratio (peak $I_{Ba}/C_m^{3/2}$). The correlation coefficient was $r = 0.022$. (*B*) I_{Ba} elicited by a test pulse to the reversal potential (+65 mV), following a 2-s conditioning pulse that elicited maximal I_{Ba}. The conditioned current is shown superimposed to the reference current, elicited without conditioning. Conditioned and reference currents were both nil during the test pulse.

nated when it chelates metal cations, with consequent acidification (Jong et al., 1993). Therefore, one possible mechanism of fast inactivation was channel closure due to acidification. Against this possibility we found that the fast phase of decay was present even when intracellular pH was buffered with 100 mM HEPES (data not shown). We also compared rates of I_{Ba} decay in cells dialyzed with 0.5, 1, 10, or 20 mM of EGTA. The rapidly decaying component was present in all and its kinetics changed only slightly (data not shown). These observations again rule out accumulation, as well as other possible mechanisms involving EGTA in the development of fast current decay.

Fast Inactivation of I_{Ba} Is a Property of the α_1 Subunit

To test whether fast inactivation depended on certain auxiliary subunits or other properties of the expression system, experiments were carried out with different combinations of subunits α_{1C}, β_{2a}, and $\alpha_2\delta$, and with native rabbit ventricular myocytes. As illustrated in Fig. 7, both phases of I_{Ba} decay were present in all cases, in-

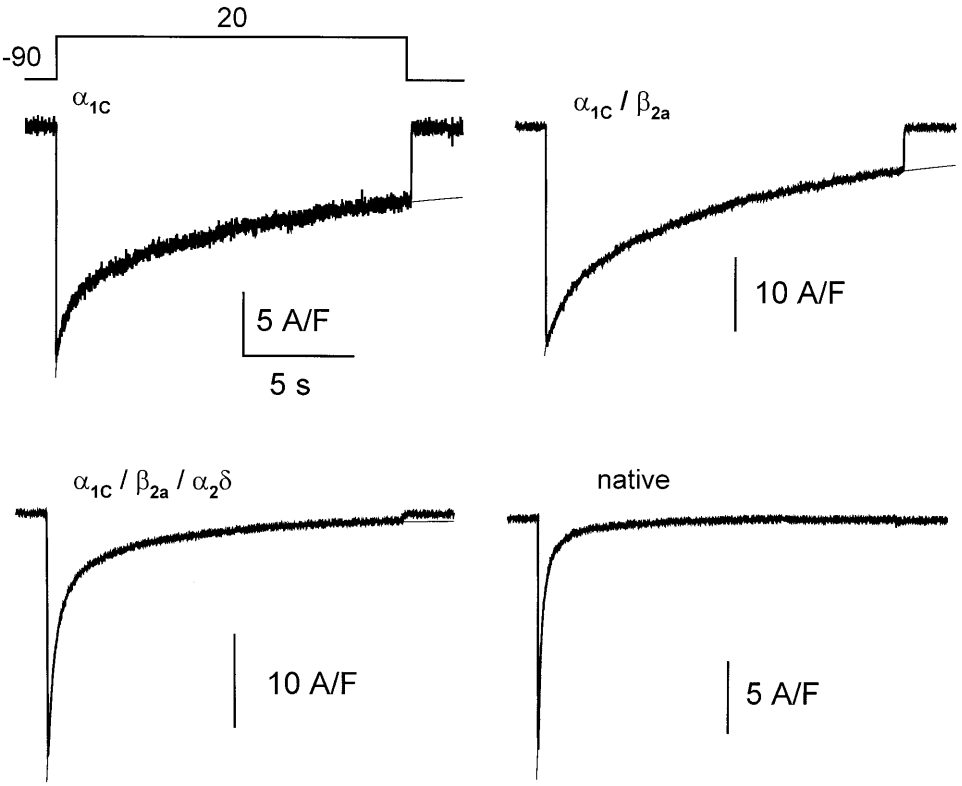

FIGURE 7. Kinetics of I_{Ba} with different combinations of subunits and in ventricular myocytes. Ba^{2+} currents elicited by 16.5-s pulses to +20 mV, in tsA201 cells transfected with cDNA combinations listed in each panel, and in a rabbit ventricular myocyte (native).

TABLE I

Composition	Number of cells	A_{fast}	A_{slow}	B	τ_{fast}, (s)	τ_{slow}, (s)
α_{1C}	6	0.35 ± 0.05	0.45 ± 0.03	0.20 ± 0.03	0.57 ± 0.06	6.88 ± 0.66
α_{1C}/β_{2a}	19	0.54 ± 0.04	0.39 ± 0.04	0.07 ± 0.02	0.65 ± 0.07	6.21 ± 0.81
$\alpha_{1C}/\beta_{2a}/\alpha_2\delta$	16	0.58 ± 0.04	0.37 ± 0.03	0.05 ± 0.03	0.58 ± 0.06	5.15 ± 0.55
native	3	0.67 ± 0.06	0.28 ± 0.04	0.04 ± 0.01	0.21 ± 0.01	1.78 ± 0.18

Two-exponential fits to I_{Ba} decay in tsA201 cells transfected with different combinations of L-type Ca^{2+} channel subunits, and in rabbit ventricular myocytes. I_{Ba} was elicited by 16.5-s long pulse from the holding potential of −90 mV to +20 mV. The fit function and parameters are described in METHODS.

cluding cells transfected with α_1 alone. The parameters of two-exponential fits and their averages are listed in Table I.

Although cells co-transfected with $\alpha_{1C} + \beta_{2a}$ had much higher current density than cells transfected with α_{1C} alone, the rates of inactivation were similar in both groups, consistent with the previous observation that β_{2a}, is the least potent among other cloned β subunits in acceleration of inactivation (De Waard and Campbell, 1995). A_{fast} increased significantly with the number of subunits, being maximal for the native channels. The kinetics of fast inactivation did not depend on the composition of the expressed channels, being in all cases about threefold slower than in native channels. The rate of the slow component increased with the number of subunits. This change was marginally significant between α_{1C} and $\alpha_{1C}/\beta_{2a}/\alpha_2\delta$ cells (at a level $P < 0.09$) and not significant between α_{1C}/β_{2a} and $\alpha_{1C}/\beta_{2a}/\alpha_2\delta$ cells. (The histogram of slow time constants of the $\alpha_{1C}/\beta_{2a}/\alpha_2\delta$ cells was bimodal, with approximately one quarter of the $\alpha_{1C}/\beta_{2a}/\alpha_2\delta$ cells centered at about the same modal value as the α_{1C}/β_{2a} group. It is possible that a group of $\alpha_{1C}/\beta_{2a}/\alpha_2\delta$ cells expressed little of the $\alpha_2\delta$ subunit or that the subunit did not incorporate stoichiometrically to the complex [Gurnett et al., 1996]. Therefore, the $\alpha_2\delta$ subunit may have had a greater effect than that reflected by our averaged measurements.)

The presence of both decay phases with every combination of subunits indicates that both inactivation mechanisms are determined by the α_{1C} subunit. That the relative amplitudes and kinetics of the two phases varied with the subunit composition is consistent with a modulatory role of the auxiliary subunits (Catterall, 1995).

DISCUSSION

The present study was designed to compare inactivation of ionic and gating currents of L-type Ca^{2+} channels in the simplest possible situation. The tsA201 cells provided a system essentially devoid of other channels. Use of Ba^{2+} as current carrier was expected to eliminate the current-dependent inactivation mechanism. In spite of these conditions, inactivation of ionic current was found to follow two kinetic phases, of which only the slow one was co-temporal with the observed single exponential reduction of gating charge. The fast phase was current-dependent and did not correlate with the reduction of the gating charge. Because the two kinetic phases of inactivation of I_{Ba} were seen in cells transfected with the α_{1C} subunit, alone, in combination with β_{2a} or with β_{2a} and $\alpha_2\delta$, as well as in rabbit ventricular myocytes, they must be a property of the α_1 subunit, depending on neither the auxiliary subunits nor the expression system. In this section we analyze the present findings, compare them with published observations and infer that the fast phase of decay is caused by Ba^{2+} binding to the channel's Ca^{2+}-inactivation site.

The Population of Ca^{2+} Channels Was Homogeneous

Ba^{2+} currents through L-type Ca^{2+} channels have been observed to decay in two phases in many different preparations. In neurons, two components of decay were observed, but the significance of the observation was obscured by the existence of multiple types of high voltage-activated Ca^{2+} channels (Boland and Digledine, 1990; Kay, 1991). In cardiac myocytes, the presence of two components of inactivation of I_{Ba} was interpreted as due to two different processes of voltage-dependent inactivation, because inactivation of I_{Ba} was believed to be purely voltage dependent (Kass and Sanguinetti, 1984; Lee et al., 1985; Boyett et al., 1994). This view could not be tested rigorously because in cardiac myocytes it is difficult to correlate inactivation of I_{Ba} with inactivation of gating currents, due to the contribution of other channels to charge movement (Bean and Ríos, 1989; Shirokov et al., 1992). These problems may have been circumvented in the present work, provided that the Ca^{2+} channels expressed in a mammalian cell line after transfection were a single population, homogeneous in its biophysical properties. This seems to have been the case, for the three following reasons:

No sizable Ca^{2+} or Ba^{2+} currents were recorded in mock-transfected cells. In our experiments, amplitudes of endogenous currents (<0.5 A/F) were always one or two orders of magnitude smaller than those in transfected cells. Therefore, the bulk of the Ba^{2+} or Ca^{2+} current in transfected tsA201 cells was probably conducted through recombinant channels, and endoge-

nous currents could not have been the reason for the multiplicity of inactivation phases.

In agreement with Kamp et al. (1996) and Josephson and Varadi (1996), we found a consistent correlation between the amount of intramembranous mobile charge and the ionic current density, suggesting that a major fraction of expressed channels function to carry current.

When rundown reduced ion current amplitude, the relative magnitudes of the two inactivation phases were conserved. Had the processes taken place in two different sets of channels, their proportions would not have been likely to remain constant during rundown.

Assuming that the population of channels was homogeneous, the question that then arises is if the kinetic phases of inactivation correspond to two different mechanisms.

Ba^{2+}-dependent Inactivation Caused the Fast Decay of Current

The fast decay of current depended on the current through the channel, rather than the applied voltage. This was demonstrated by three observations:

In experiments with a double pulse protocol, current availability depended on the voltage of the conditioning pulse in a U-shaped manner, and inactivation reached a maximum at voltages that made inward current greatest, much as has been described for Ca^{2+}-dependent inactivation (Eckert and Chad, 1984). In the present experiments the observation was free from many errors that may have obscured this property in previous studies with native cardiomyocytes. Although a U-shaped voltage dependence is expected in current-dependent processes, it could also arise from (voltage-dependent) potentiation, that offsets the inactivation effect at high voltages (Lee, 1987). Voltage-dependent potentiation cannot explain the present observations because current elicited by the test after a high voltage conditioning pulse was never greater than reference, and its kinetics remained the same. Our failure to observe voltage-dependent potentiation agrees with the report of Cens et al. (1996) that β_{2a} failed to promote voltage-dependent potentiation, at variance with the effects of other types of β subunit.

Recovery of I_{Ba} from inactivation was slower after a conditioning to +20 mV than to +60 mV (data not shown). Much more Ba^{2+} enters the cell during a pulse to +20 than at +60 mV. The longer lasting inactivation induced at +20 mV may simply be a consequence of the persistence of inactivating concentrations of Ba^{2+} near the channels for a longer time (as argued by Kay, 1991, for Ca^{2+} currents in neurons).

There was no immobilization or voltage shift of gating current with kinetics corresponding to those of the fast decay of ionic current. In the current view, inactivation of Na^+ and K^+ channels acquires its voltage dependence indirectly, through a link to channel opening. In Na^+ and K^+ channels inactivation is more likely to happen when gating particles are in the activating position. In a microscopically reversible system, this implies that inactivation stabilizes the voltage sensor in its activating position, negatively shifting the transition voltage of gating currents and reducing the availability of charge mobile in the range of voltages that normally cause activation. This was not found in our case for the fast component of inactivation of I_{Ba}.

The observed decay of I_{Ba} could not have been due to bulk accumulation or cell loading by the permeating Ba^{2+}, as the effect failed to correlate with the geometry of the cell (Fig. 6 *A*), and Ba^{2+} entry during long-lasting depolarization failed to change the reversal potential of the current (Fig. 6 *B*). This conclusion is also consistent with the finding (Cavalié et al., 1983) that the amplitude of single channel current remains the same during prolonged depolarization. The decay can therefore be attributed to an inactivation gating process, dependent on the local increase of $[Ba^{2+}]$, at levels that do not significantly change the driving force for I_{Ba}.

The evidence strongly favors a mechanism that requires binding of Ba^{2+} to a site on the channel molecule. Most importantly, the fast decay of Ca^{2+} channel current was absent when Na^+ carried the current, even at high current densities. This fact is further evidence against an accumulation phenomenon, which would not be expected to work solely for Ba^{2+}. Furthermore, because I_{Ba} in α_1 cells exhibits the fast decay, the putative Ba^{2+} site has to be on the α_1 polypeptide. That the fast decay was observed in currents carried by Ba^{2+}, by Ca^{2+}, and by Na^+ in the presence of extracellular Ca^{2+}, suggests that Ba^{2+} causes inactivation by binding to the Ca^{2+}-inactivation site. That fast inactivation of Ba^{2+} current occurred without correlative changes in gating current is consistent with this hypothesis, considering that the voltage-dependent and the Ca^{2+}-dependent mechanisms of inactivation do not interact (Hadley and Lederer, 1991; Shirokov et al., 1993).

Previous work has failed to clarify whether or not I_{Ba} inactivates by an ion-dependent mechanism. McDonald et al. (1986) did not find U-shaped voltage dependence for inactivation of Ba^{2+} currents in on-cell patches of guinea pig ventricular myocytes. On the same preparation, Imredy and Yue (1994) saw some reduction in the extent of decay of single channel I_{Ba} at voltages above +20 mV, and tentatively interpreted it as evidence of Ba^{2+}-dependent inactivation. Mazzanti et al. (1991) found fast decay of Ba^{2+} current provided that there were multiple channels in a patch, and proposed a Ba^{2+}-dependent mechanism of inactivation enhanced by channel clustering. The interpretation of

single channel on-cell measurements is complicated by the possibility of inactivation by Ca^{2+} released from intracellular stores (Galli et al., 1994; Sham et al., 1995). Schneider et al. (1991) found that entry of Ba^{2+} into smooth muscle cells through ATP-activated channels reduced whole-cell L-type channel Ba^{2+} currents by about 20%. Perfusion of rabbit portal vein smooth muscle cells with 100 μM of Ba^{2+} in the patch pipette led to a 10% reduction of I_{Ca} (Ohya et al., 1987). The results are consistent with a finding of Brown et al. (1981) that perfusion of *Helix aspersa* neurons with 1 mM Ba^{2+} in the pipette reduced I_{Ba} by some 20%. In sum, the evidence with single channels is inconclusive, while in whole cells there are modest effects of perfusion with Ba^{2+}. These results do not rule out inactivation by the high concentrations of Ba^{2+} that are likely to occur at the putative site, which is presumably located near the channel mouth (De León et al., 1995).

The main characteristics of Ca^{2+}-dependent inactivation of I_{Ca} were previously reproduced with a simple three-gate model of the L-type channel (Shirokov et al., 1993). We now show that this model also accounts for the properties of I_{Ba}, assuming that Ba^{2+} substitutes for Ca^{2+} at the inactivation site. The model includes voltage-dependent properties, activation, and inactivation, which are independent of cation binding, and are represented in SCHEME I:

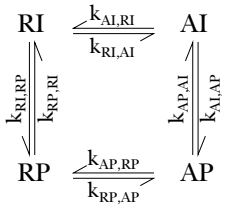

(SCHEME I)

Activation is the opening of a voltage-operated gate, whose states are resting (R) and activated (A). Voltage-dependent inactivation involves a second gate, with a permissive (P) and an inactivated state (I). The P → I transition is not intrinsically voltage-dependent, but is favored from channel state AP.[1]

Ion-dependent inactivation is pictured by a third gate, the states of which are represented in SCHEME II:

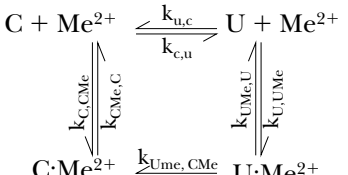

(SCHEME II)

The ion-controlled gate can be "covering" (C, channel closed) or "uncovering" (U). Me^{2+}, normally Ca^{2+}, inactivates the channel because its binding stabilizes state C, that is, the equilibrium between $C:Me^{2+}$ and $U:Me^{2+}$ is shifted toward $C:Me^{2+}$. Accordingly, and to satisfy microscopic reversibility, the affinity of the site must be greater in state C than in state U. The channel state is described by the state of its three gates and is open only in state APU.[2] The ion-dependent inactivation process does not affect the voltage-dependent processes in any way (implying that the evolution of states depicted in SCHEME I can be solved independently), while the states in SCHEME II are influenced by the voltage-dependent gates only because the concentration of the current-carrying ion changes when the channel opens. $[Me^{2+}]$ at the site was assumed to be an instantaneous function of the channel current i, defined as: $[Me^{2+}]_{bulk} + i/4\pi FDr$, where $[Me^{2+}]_{bulk}$ is 50 nM, F is the faraday, the diffusion constant D is 10^{-6} cm^2s^{-1}, and the distance r from the channel mouth to the binding site is 1 nm.

In this model, dissociation constants (K_d) for Ca^{2+} are supposed to be 1 μM in state C and 100 μM in state U. I_{Ba} was simulated assuming 100-fold higher K_ds in both states (which was achieved by reducing the binding rate constants). The only other difference between the two ions was a two-times greater single channel current for Ba^{2+} at any given extracellular $[Me^{2+}]$.[3]

The simulations[4] are illustrated in Fig. 8, where current records, exponential fits, and fit parameters are shown in a manner similar to Fig. 1. With this choice of parameters the model reproduced well the main properties of I_{Ba}, including: the presence of two kinetic

[1]The horizontal transitions in SCHEME I are voltage dependent, with rate constant $k_{RP,AP} = \mathbf{a}_1 \exp\{(V - V_1)/2K - b[(V - V_1)/2K]^2\}$, where V_1 is a transition voltage and K a steepness factor, the rate constant of the reverse transition is equal to $k_{RP,AP} \exp\{(V_1 - V)/K\}$, and the rate constants between states RI and AI were calculated similarly, with $\mathbf{a}_2$ and V_2 substituted for $\mathbf{a}_1$ and V_1. $\mathbf{a}_1 = 100\ s^{-1}$, $\mathbf{a}_2 = 33\ s^{-1}$, $V_1 = 0$ mV, $V_2 = -80$ mV, K = 8 mV, and b = 0.1. The inactivation rate constants were: $k_{AP,AI} = 0.15\ s^{-1}$, $k_{AI,AP} = 0.05\ s^{-1}$. The rates of recovery from inactivation were set to satisfy kinetics of recovery, $k_{RP,RI} + k_{RI,RP} = 20\ s^{-1}$, and microscopic reversibility, $k_{RI,RP}/k_{RP,RI} = (k_{AP,AI}/k_{AI,AP}) \exp[(V_1 - V_2)/2K]$.

[2]Parameters of SCHEME II were: $k_{CMe,C} = 1\ s^{-1}$, $k_{UMe,U} = 0.01\ s^{-1}$, $k_{C,U} = 100\ s^{-1}$, $k_{U,C} = 1{,}000\ s^{-1}$, $k_{UMe,CMe} = 1{,}000\ s^{-1}$, $k_{CMe,UMe} = 1\ s^{-1}$. $k_{C,CMe} = k_{U,UMe} = 10^6\ M^{-1}s^{-1}$ for Ca^{2+} and $10^4\ M^{-1}s^{-1}$ for Ba^{2+}.

[3]Single channel currents in Ba^{2+} and Ca^{2+} were 0.6 and 0.3 pA, respectively, at 20 mV and saturating $[Me^{2+}]_e$. At other voltages and $[Me^{2+}]_e = 10$ mM, the amplitude of single channel current was calculated as $XV\{(\exp[-V/12\ mV])/(1 - \exp[(-V/12\ mV])\} \times \{[Me^{2+}]_e/([Me^{2+}]_e + 14\ mM)\}$, where X is 0.08 pA for Ca^{2+} and 0.16 pA for Ba^{2+}.

[4]Total current was calculated as $N \times P_o \times i$, where P_o is the probability that the three gates are in their permissive states. N was 125,000, corresponding to ≈25 channels/μm² in a cell of $C_m = 50$ pF. The channels generated both ionic and gating currents, in parallel with C_m and in series with resistance $R_s = 5$ MΩ. (The computer program can be obtained by E-mail requests to rshiroko@rush.edu)

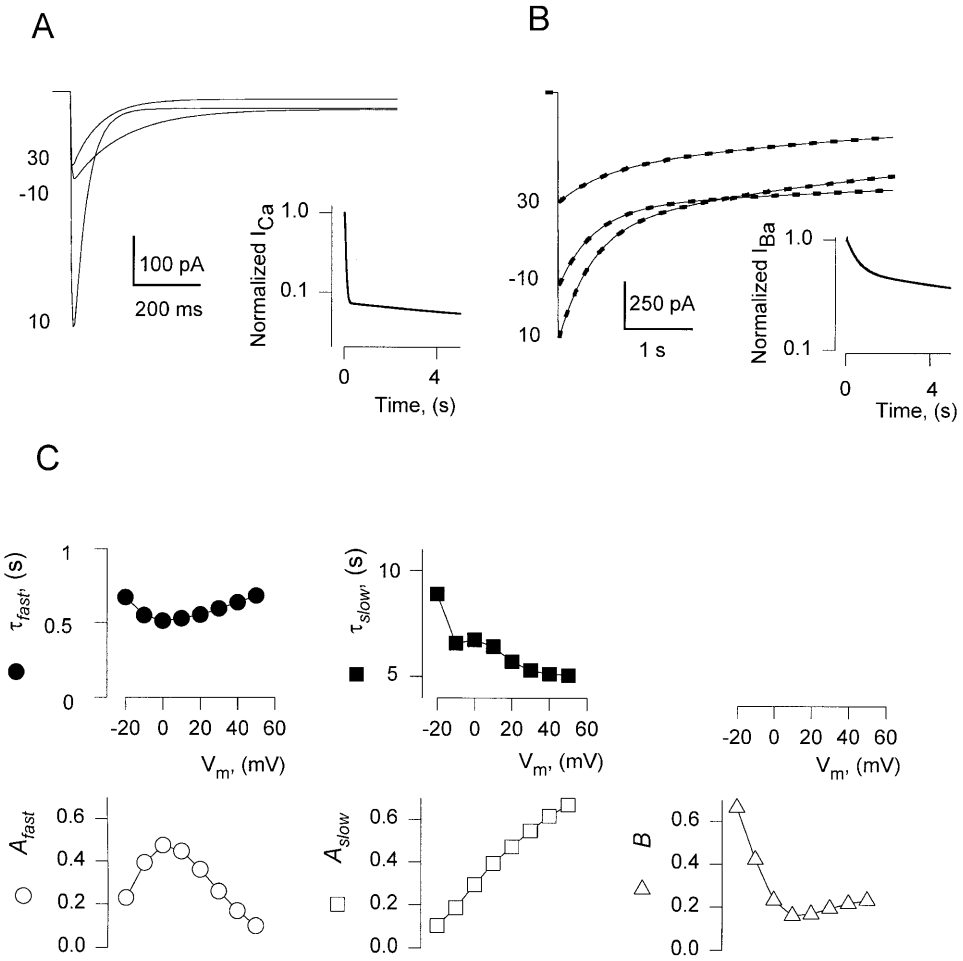

FIGURE 8. A model of Ca^{2+}-dependent inactivation can also describe Ba^{2+}currents. Simulations with the model described in the text, presented and analyzed in the same order as the experimental records in Fig. 1. (*A*) Simulated I_{Ca} elicited by pulses from −90 mV to voltages indicated near the traces. (*inset*) Simulated I_{Ca} at 0 mV, normalized to the peak value and plotted in semilog scale. (*B*) Simulated I_{Ba} during long duration pulses to voltages indicated. *Dashed lines*: two-exponential fits. (*inset*) Simulated I_{Ba} at 0 mV, normalized to the peak value and plotted in semilog scale. (*C*) Parameters of two-exponential fits to the simulated I_{Ba}.

phases of inactivation, the voltage dependence of τ_{slow}, the amplitudes of all components, and the fact that τ_{fast} was steeply voltage-dependent for I_{Ca} (Fig. 8 *A*) but not I_{Ba} (Fig. 8 *B*).

Voltage-dependent Inactivation Underlies the Slow Phase of Current Decay

The present results include a reduction in the amount of charge available to move above −60 mV, upon prolonged depolarization. This reduction, which depends exponentially on duration of the depolarizing pulse, is cotemporal with the slow phase of current decay, regardless of the ion that carries the current. This implies that the slow phase of decay of I_{Ba} is the result of voltage-dependent inactivation. The concomitant reduction in the availability of gating charge could be the consequence of two not mutually exclusive mechanisms: charge immobilization associated with inactivation (Armstrong and Bezanilla, 1977), or a negative shift in the voltage distribution of intramembrane mobile charge, similar to that accompanying slow inactivation of squid Na^+ channels (Bezanilla et al., 1982), inactivation of the voltage sensor of skeletal muscle (Brum et al., 1988), and inactivation of L-type channels in guinea pig cardiomyocytes (Shirokov et al., 1992) and embryonic chick ventricular myocytes (Josephson, 1996).

Implications for Other Ca^{2+} Channel Studies

The present results define two kinetic components of decay of Ba^{2+} currents through Ca^{2+} channels, show that the slow phase, with characteristic times of seconds, is caused by voltage-dependent inactivation, and suggest binding of Ba^{2+} as probable cause for the fast phase. These findings call into question the widespread use of Ba^{2+} currents as tools to quantify purely voltage-dependent processes in Ca^{2+} channels. By showing the close association between gating current inactivation and a decay of current that takes place in seconds, it forces reconsideration of studies that attribute decay phases of hundreds of ms to voltage-dependent processes.

For example, Zong et al. (1994), in their study of L-type Ca^{2+} channels in HEK 293 cells, used the difference between the "slow" time constant (~200 ms) in a two-

exponential fit to I_{Ca} elicited by 400-ms pulses, and the time constant in a single exponential fit to I_{Ba} (~300 ms) to argue that Ca^{2+} may make voltage-dependent inactivation faster. Clearly the time constants were too short (and so were the applied pulses) to significantly explore the voltage-dependent process, which we now show to be much slower.

Zhang et al. (1994) analyzed the kinetics of I_{Ba} through chimeric channels in *Xenopus* oocytes to localize determinants of voltage-dependent inactivation. In this study, an α_{1A} (a putatively P/Q-type channel from brain) with relatively slow rate of I_{Ba} decay was chimerized with the rapidly inactivating α_{1E} (doe-1, marine ray). The work unquestionably localized the determinants of subunit-specific differences in decay of I_{Ba} to segment IS6 and its vicinity. Because the inactivation of I_{Ba} in doe-1 is believed to be exclusively voltage dependent (Ellinor et al., 1993), the rates of decay found in the rapidly inactivating chimeras, 10–30 s^{-1}, were naturally attributed to voltage-dependent inactivation. However, P-type channels are susceptible to Ca^{2+}-dependent inactivation (Tareilus et al., 1994), and therefore the assertion that fast inactivation in the chimeras is voltage-dependent should be supported with the use of longer pulses or other tests.

Possible involvement of the first domain in determining the rate of I_{Ba} decay was also demonstrated by Parent et al. (1995) working with a chimera of α_{1C} and α_{1S}. Even though the demonstration was clear, the conclusion that the first repeat affects voltage-dependent inactivation can be criticized on similar grounds, because it relies on the assumption that I_{Ba} inactivation is exclusively voltage-dependent.

In conclusion, the identification of structural determinants of voltage-dependent inactivation in Ca^{2+} channels can not be based solely on the analysis of I_{Ba}, since the ability to induce inactivation of the L-type Ca^{2+} channel appears not to be a unique property of Ca^{2+} ions. The main consequence of the present work is to require careful reconsideration of the mechanisms attributed to inactivation in previous and future studies.

The tsA201 cell lines were a gift of Dr. M.M. Hosey (Northwestern University, Chicago, IL). The L-type Ca^{2+} channels cDNA sequences were gifts of Drs. E. Perez-Reyes (Loyola University, Maywood, IL) and M.M. Hosey. We thank Andy Chien, Tipu Puri and M.M. Hosey (Northwestern) for supplying the rabbit cardiomyocytes.

This work was supported in part by National Institutes of Health Grant AR 43113 and a Grant-in-Aid from the American Heart Association (to E. Ríos) and by grants from the American Heart Association of Metropolitan Chicago (to R. Shirokov).

Original version received 30 October 1996 and accepted version received 16 January 1997.

REFERENCES

Armstrong, C.M., and F. Bezanilla. 1977. Inactivation of the sodium channel. II. Gating current experiments. *J. Gen. Physiol.* 70:567–590.

Bean, B.P., and E. Ríos. 1989. Nonlinear charge movement in mammalian cardiac ventricular cells. Components from Na^+ and Ca^{2+} channel gating. *J. Gen. Physiol.* 94:65–93.

Bezanilla, F., R.E. Taylor, and J. Fernandez. 1982. Distribution and kinetics of membrane dielectric polarization. I. Long-term inactivation of gating currents. *J. Gen. Physiol.* 79:21–40.

Boland, L., and R. Dingledine. 1990. Multiple components of both transient and sustained barium currents in a rat dorsal root ganglion cell line. *J. Physiol. (Lond.).* 420:223–245.

Boyett, M.R., H. Honjo, S.M. Harrison, W.-J. Zang, and M.S. Kirby. 1994. Ultra-slow voltage dependent inactivation of the calcium current in guinea-pig and ferret ventricular myocytes. *Pflüg. Arch.* 428:39–50.

Brehm, P., and R. Eckert. 1978. Calcium entry leads to inactivation of calcium channel in Paramecium. *Science (Wash. DC).* 202:1203–1206.

Brown, A.M., K. Morimoto, Y. Tsuda, and D.L. Wilson. 1981. Calcium current-dependent and voltage-dependent inactivation of calcium channels in *Helix aspersa*. *J. Physiol. (Lond.).* 320:193–218.

Brum, G., R. Fitts, G. Pizarro, and E. Ríos. 1988. Voltage sensors of the frog skeletal muscle membrane require calcium to function in excitation-contraction coupling. *J. Physiol. (Lond.).* 398:475–505.

Catterall, W. 1995. Structure and function of voltage-gated ion channels. *Annu. Rev. Biochem.* 64:493–531.

Cavalie, A., R. Ochi, D. Pelzer, and W. Trautwein. 1983. Elementary currents through Ca^{2+} channels in guinea-pig myocytes. *Pflüg. Arch.* 405:284–297.

Cens, T., M. Mangoni, S. Richard, J. Nargeot, and P. Charnet. 1996. Coexpression of the β_2 subunit does not induce voltage-dependent facilitation of the class C L-type Ca channel. *Pflüg. Arch.* 431: 771–774.

Cox, D.H., and K. Dunlap. 1994. Inactivation of N-type calcium current in chick sensory neurons: calcium and voltage dependence. *J. Gen. Physiol.* 104:311–336.

Chien, A., X. Zhao, R. Shirokov, T. Puri, C.F. Chang, D. Sun, E. Ríos, and M. Hosey. 1995. Roles of membrane-localized β subunit in the formation and targeting of functional L-type Ca^{2+} channels. *J. Biol. Chem.* 270:30036–30044.

De Leon, M., Y. Wang, L. Jones, E. Perez-Reyes, X. Wei, T. Wah Soong, T.P. Snutch, and D.T. Yue. 1995. Essential Ca^{2+}-binding motif for Ca^{2+}-sensitive inactivation of L-type Ca^{2+} channels. *Science (Wash. DC).* 270:1502–1506.

De Waard, M., and K. Campbell. 1995. Subunit regulation of neuronal α_{1A} Ca^{2+} channels expressed in *Xenopus* oocytes. *J. Physiol. (Lond.).* 485:619–634.

Eckert, R., and J.E. Chad. 1984. Inactivation of Ca channels. *Prog. Biophys. Mol. Biol.* 44:215–267.

Ellinor, P.T., J.-F. Zhang, A.D. Randall, M. Zhou, T.L. Schwarz, R.W. Tsien, and W.A. Horne. 1993. Functional expression of a rapidly inactivating neuronal calcium channel. *Nature (Lond.).* 363:455–458.

Field, A., C. Hill, and G. Lamb. 1988. Asymmetric charge movement and calcium currents in ventricular myocytes of neonatal rat. *J. Physiol. (Lond.).* 406:277–297.

Fox, A.P. 1981. Voltage-dependent inactivation of a calcium chan-

nel. *Proc. Natl. Acad. Sci. USA*. 78:953–956.

Galli, A., A. Ferroni, L. Bertollini, and M. Mazzanti. 1994. Inactivation of single Ca^{2+} channels in rat sensory neurons by extracellular Ca^{2+}. *J. Physiol. (Lond.)*. 477:15–26.

Gurnett, C., M. De Waard, and K. Campbell. 1996. Dual function of the voltage-dependent Ca^{2+} channel $\alpha_2\delta$ subunit in current stimulation and subunit interaction. *Neuron*. 16:431–440.

Hadley, R.W., and J.R. Hume. 1987. An intrinsic potential-dependent inactivation mechanism associated with calcium channels in guinea-pig myocytes. *J. Physiol. (Lond.)*. 389:205–222.

Hadley, R.W., and W.J. Lederer. 1989. Intramembrane charge movement in guinea-pig and rat ventricular myocytes. *J. Physiol. (Lond.)*. 415:601–624.

Hadley, R.W., and W.J. Lederer. 1991. Ca^{2+} and voltage inactivate Ca^{2+} channels in guinea-pig ventricular myocytes through independent mechanisms. *J. Physiol. (Lond.)*. 444:257–268.

Harafuji, H., and Y. Ogawa. 1980. Re-examination of the apparent binding constant of ethylene glycol bis(-aminoethyl ether)-N,N,N′,N′-tetraacetic acid with calcium around neutral pH. *J. Biochem*. 87:1305–1312.

Hess, P., J. Lansman, and R.W. Tsien. 1986. Calcium channel selectivity for divalent and monovalent carions. Voltage and concentration dependence of single channel current in ventricular heart cells. *J. Gen. Physiol*. 88:293–319.

Heyer, C.B., and H.D. Lux. 1976. Properties of a facilitating calcium current in pace-maker neurones of the snail *Helix pomatia*. *J. Physiol. (Lond.)*. 88:319–348.

Hoel, P.G. 1971. Introduction to Mathematical Statistics. Fourth Edition. John Wiley & Sons, Inc. New York. 211–217.

Hoshi, T., J. Rothlein, and S.J. Smith. 1984. Facilitation of Ca^{2+} channel currents in bovine adrenal chromaffin cells. *Proc. Natl. Acad. Sci. USA*. 81:5871–5875.

Hui, C.S., and W.K Chandler. 1990. Intramembranous charge movement in frog cut twitch fibers mounted in a double Vaseline-gap chamber. *J. Gen. Physiol*. 96:257–298.

Imoto, Y., T. Ehara, and M. Goto. 1985. Calcium channel currents in isolated guinea-pig ventricular cells superfused with Ca-free EGTA solution. *Jpn. J. Physiol*. 35:917–932.

Imredy, J.P., and D.T. Yue. 1992. Submicroscopic Ca^{+2} diffusion mediates inhibitory coupling between individual Ca^{+2} channels. *Neuron*. 9:197–207.

Imredy, J.P., and D.T. Yue. 1994. Mechanism of Ca^{+2}-sensitive inactivation of L-type Ca^{+2} channels. *Neuron*. 12:1301–1318.

Jong, D.-S., P.C. Pape, W.K. Chandler, and S.M. Baylor. 1993. Reduction of calcium inactivation of sarcoplasmic reticulum calcium release by fura-2 in voltage-clamped cut twitch fibers from frog muscle. *J. Gen. Physiol*. 102:333–370.

Josephson, I. 1996. Depolarization shifts the voltage dependence of cardiac sodium channel and calcium channel gating charge movements. *Pflüg. Arch*. 431:895–904.

Josephson, I., and G. Varadi. 1996. The β subunit increases Ca^{2+} currents and gating charge movements of human cardiac L-type Ca^{2+} channels. *Biophys. J*. 70:1285–1293.

Kaibara, M., and M. Kameyama. 1988. Inhibition of the calcium channel by intracellular protons in single ventricular myocytes of the guinea-pig. *J. Physiol. (Lond.)*. 403:621–640.

Kamp, T., M.T. Perez-Garcia, and E. Marban. 1996. Enhancement of ionic current and charge movement by coexpression of calcium channel β_{1A} subunit with α_{1C} subunit in a human embryonic kidney cell line. *J. Physiol. (Lond.)*. 492:89–96.

Kass, R.S., and M.C. Sanguinetti. 1984. Inactivation of calcium channel current in the calf cardiac Purkinje fiber. *J. Gen. Physiol*. 84:705–726.

Kay, A.R. 1991. Inactivation kinetics of calcium current of accutely dissociated CA1 pyramidal cells of the mature guinea-pig hippocampus. *J. Physiol. (Lond.)*. 437:27–48.

Kostyuk, P.G., S.L. Mironov, and Y.M. Shuba. 1983. Two ion selecting filters in the calcium channel of the somatic membrane of mollusc neurons. *J. Membr. Biol*. 76:83–93.

Lee, K.S. 1987. Potentiation of the calcium channel currents of internally perfused mammalian heart cells by repetitive depolarization. *Proc. Natl. Acad. Sci. USA*. 84:3941–3945.

Lee, K.S., E. Marban, and R.W. Tsien. 1985. Inactivation of calcium channels in mammalian heart cells: joint dependence on membrane potential and intracellular calcium. *J. Physiol. (Lond.)*. 364:395–411.

Mazzanti, M., L.J. DeFelice, and Y.M. Liu. 1991. Gating of L-type Ca^{2+} channels in embrionic chick ventricle cell: dependence on voltage, current and channel density. *J. Physiol. (Lond.)*. 443:307–344.

McDonald, T.F., A. Cavalié, W. Traurwein, and D. Pelzer. 1986. Voltage-dependent properties of macroscopic and elementary calcium channel currents in guinea pig ventricular myocytes. *Pflüg. Arch*. 406:437–448.

Mitra, R., and M. Morad. 1985. A uniform enzymatic method for dissociation of myocytes from hearts and stomachs of vertebrates. *Am. J. Physiol*. 249:H1056–H1060.

Neely, A., R. Olcese, X. Wei, L. Birnbaumer, and E. Stefani. 1994. Ca^{2+}-dependent inactivation of a cloned cardiac Ca^{2+} channel α_{1C} subunit (α_{1C}) expressed in *Xenopus* oocytes. *Biophys. J*. 66: 1895–1903.

Neher, E. 1986. Concentration profiles of intracellular Ca^{2+} in the presence of diffusible chelator. *Exp. Brain Res. Ser*. 14:80–96.

Ohya, Y., K. Kitamura, and H. Kuriyama. 1987. Regulation of calcium current by intracellular calcium in smooth muscle cells of rabbit portal vein. *Circ. Res*. 62:375–383.

Parent, L., M. Gopalakrishnan, A.E. Lacerda, X. Wei, and E. Perez-Reyes. 1995. Voltage-dependent inactivation in a cardiac-skeletal chimeric calcium channel. *FEBS Lett*. 360:144–150.

Schneider, P., H.H. Hopp, and G. Isenberg. 1991. Ca^{2+} influx through ATP-gated channels increments $[Ca^{2+}]_i$ and inactivates I_{Ca} in myocytes from guinea-pig urinary bladder. *J. Physiol. (Lond.)*. 440:479–496.

Sculptoreanu, A., T. Scheuer, and W. Catterall. 1993. Voltage-dependent potentiation of L-type Ca^{2+} channels due to phosphorylation by cAMP-dependent protein kinase. *Nature (Lond.)*. 364:240–243.

Sham, J., L. Cleeman, and M. Morad. 1995. Functional coupling of Ca^{2+} channels and ryanodine receptors in cardiac myocytes. *Proc. Natl. Acad. Sci. USA*. 92:121–125.

Shirokov, R., R. Levis, N. Shirokova, and E. Ríos. 1992. Two classes of gating current from L-type Ca channels in guinea pig ventricular myocytes. *J. Gen. Physiol*. 99:863–895.

Shirokov, R., R. Levis, N. Shirokova, and E. Ríos. 1993. Ca^{2+}-dependent inactivation of cardiac L-type Ca^{2+} channels does not affect their voltage sensor. *J. Gen. Physiol*. 102:1005–1030.

Tareilus, E., J. Schoch, and H. Breer. 1994. Ca^{2+}-dependent inactivation of P-type calcium channels in nerve terminals. *J. Neurochem*. 62:2283–2291.

Tillotson, D. 1979. Inactivation of Ca conductance dependent on entry of Ca ions in molluscan neurons. *Proc. Natl. Acad. Sci. USA*. 77:1497–1500.

Tsien, R.W., and R.Y. Tsien. 1990. Calcium channels, stores, and oscillations. *Annu. Rev. Cell. Biol*. 6:715–760.

Turner, P., T. Westwood, C. Regen, and R. Steinhardt. 1988. Increased protein degradation results from elevated free calcium levels found in muscle from *mdx* mice. *Nature (Lond.)*. 335:735–738.

Zhang, J.-F., P. Ellinor, R. Aldrich, and R. Tsien. 1994. Molecular determinants of voltage-dependent inactivation in calcium channels. *Nature (Lond.)*. 372:97–100.

Zong, S., J. Zhou, and T. Tanabe. 1994. Molecular determinants of calcium-dependent inactivation in cardiac L-type calcium channels. B.B.R.C. 201:117–123.